JHR 83: 73–99 (2021)
doi: 10.3897/jhr.83.64018
https://jhr.pensoft.net

RESEARCH ARTICLE

JOURNAL OF Hymenoptera RESEARCH
A peer-reviewed open-access journal
The International Society of Hymenopterists

Ovipositor of the braconid wasp *Habrobracon hebetor*: structural and functional aspects

Michael Csader[1], Karin Mayer[1], Oliver Betz[1], Stefan Fischer[1,2], Benjamin Eggs[1]

1 *Evolutionary Biology of Invertebrates, Institute of Evolution and Ecology, University of Tübingen, Auf der Morgenstelle 28, 72076, Tübingen, Germany* **2** *Tübingen Structural Microscopy Core Facility (TSM), Center for Applied Geosciences, University of Tübingen, Schnarrenbergstrasse 94–96, 72076, Tübingen, Germany*

Corresponding author: Michael Csader (m.csader@web.de)

Academic editor: J. Fernandez-Triana | Received 5 February 2021 | Accepted 22 April 2021 | Published 28 June 2021

http://zoobank.org/FEA676AD-6473-4EA3-8F74-E7F83A572234

Citation: Csader M, Mayer K, Betz O, Fischer S, Eggs B (2021) Ovipositor of the braconid wasp *Habrobracon hebetor*: structural and functional aspects. Journal of Hymenoptera Research 83: 73–99. https://doi.org/10.3897/jhr.83.64018

Abstract

The Braconidae are a megadiverse and ecologically highly important group of insects. The vast majority of braconid wasps are parasitoids of other insects, usually attacking the egg or larval stages of their hosts. The ovipositor plays a crucial role in the assessment of the potential host and precise egg laying. We used light- and electron-microscopic techniques to investigate all inherent cuticular elements of the ovipositor (the female 9th abdominal tergum, two pairs of valvifers, and three pairs of valvulae) of the braconid *Habrobracon hebetor* (Say, 1836) in detail with respect to their morphological structure and microsculpture. Based on serial sections, we reconstructed the terebra in 3D with all its inherent structures and the ligaments connecting it to the 2nd valvifers. We examined the exact position of the paired valvilli, which are bilateral concave structures that protrude into the egg canal. In *H. hebetor*, these structures putatively divert the egg ventrally between the 1st valvulae for oviposition. We discuss further mechanical and functional aspects of the ovipositor in order to increase the understanding of this putative key feature in the evolution of braconids and of parasitoid wasps in general.

Keywords

3D reconstruction, Braconidae, functional morphology, Hymenoptera, parasitoid, SEM, serial sectioning, terebra

Copyright *Michael Csader et al.* This is an open access article distributed under the terms of the Creative Commons Attribution License (CC BY 4.0), which permits unrestricted use, distribution, and reproduction in any medium, provided the original author and source are credited.

Introduction

Most hymenopteran species belong to the guild of parasitoids of other insects (Quicke 1997). The astonishing radiation of the most diverse parasitoid wasp lineages (i.e. Ceraphronoidea, Ichneumonoidea and Proctotrupomorpha; = Parasitoida *sensu* Peters et al. 2017) has been estimated to have occurred 266–195 million years ago. This process was presumably triggered by continuous adaptations of the parasitoid lifestyle including features such as endoparasitism, miniaturization, and/or modifications of the ovipositor (Peters et al. 2017). Adaptations in oviposition behavior and the morphological structure of the ovipositor might not only have increased the reproductive success of the wasps, but have potentially also enabled them to oviposit in a multitude of different substrates, facilitating the acquisition of new hosts and host ranges (Gauld and Bolton 1988; Quicke 1997). The ovipositor of parasitoid wasps serves a set of functions: penetration of the substrate (if the host is concealed) or of the targeted egg/puparium, the location, assessment, and piercing of the host, the injection of venom, the killing of the competitors' eggs or larvae, the finding of a suitable place for egg laying, and oviposition (Quicke et al. 1999).

The hymenopteran ovipositor is an anatomical and functional cluster that consists of the following elements: the paired 1st valvulae (8th gonapophyses), the 2nd valvula (fused 9th gonapophyses), the paired 3rd valvulae (9th gonostyli), the paired 1st valvifers (fusion of the 8th gonocoxites and gonangula (Vilhelmsen 2000)), the paired 2nd valvifers (9th gonocoxites), and the female T9 (9th abdominal tergum) (Snodgrass 1933; Oeser 1961). All the morphological terms are applied according to the Hymenoptera Anatomy Ontology (HAO; Yoder et al. 2010; Hymenoptera Anatomy Consortium 2021; a table of the terms used and of their definitions is given in Table A1 in the Appendix 1). The 1st valvifer is connected to the 2nd valvifer via the intervalvifer articulation and with the female T9 via the tergo-valvifer articulation. Each of the 1st valvulae is attached to the corresponding 1st valvifer via the dorsal ramus of the 1st valvula, whereas the 2nd valvula is connected to the 2nd valvifer via the basal articulation and fine ventral rami of the 2nd valvula (cf. Bender 1943). Both the 1st and the 2nd valvulae are firmly interlocked along almost their entire length via a tongue and groove-like system called the olistheter. They form the terebra (= ovipositor shaft) and accommodate the egg canal (Oeser 1961; Quicke et al. 1994).

Despite many comparative studies on the terebra of hymenopterans (Snodgrass 1933; Oeser 1961; Quicke et al. 1994; LeRalec et al. 1996), the number of publications concerning the entire ovipositor is limited for the vast number of hymenopteran (super-)families. Studies that describe all the inherent cuticular elements and muscles of the ovipositor and (in part) also consider functional aspects include several basal 'symphytan' families (Smith 1970, 1972; Vilhelmsen 2000; Vilhelmsen et al. 2001), some aculeate species (i.e. *Apis melifera* Linnaeus, 1758 (Apidae) (Snodgrass 1933), species belonging to Chrysidoidea (Barbosa et al. 2021), *Sceliphron destillatoruim* (Illiger, 1807) (Sphecidae), *Ampulex compressa* (Fabricius, 1781) (Ampulicidae) (Graf et al. 2021), *Vespa crabro* Linnaeus, 1758 (Vespidae) (Stetsun and Matushkina 2020),

and species belonging to the Crabronidae (Matushkina 2011; Matushkina and Stetsun 2016; Stetsun et al. 2019) and Pompilidae (Kumpanenko and Gladun 2018)), and a few parasitoid species belonging to the Cynipoidea (Frühauf 1924; Fergusson 1988), Platygastroidea (Field and Austin 1994), Chalcidoidea (Hanna 1934; King 1962; King and Copland 1969; Copland and King 1972a, 1972b, 1972c, 1973; Copland 1976), and Ceraphronoidea (Ernst et al. 2013). The musculoskeletal ovipositor system and the actuation mechanisms of ichneumonoid wasps have been described recently in the ichneumonid *Venturia canescens* (Gravenhorst, 1829) (Eggs et al. 2018) and the braconid *Diachasmimorpha longicaudata* (Ashmead, 1905) (van Meer et al. 2020), respectively. Furthermore, drawings of the braconid ovipositor including all inherent cuticular elements exist for *Atanycolus rugosiventris* (Ashmead, 1889) (Snodgrass 1933), *Apanteles congestus* (Nees, 1834) (Oeser 1961), and *Stenobracon deesae* (Cameron, 1902) (Alam 1953; Venkatraman and Subba Rao 1954).

However, knowledge about structural and functional aspects of the ovipositor system of the ecologically and morphologically extremely diverse and species-rich Braconidae remains limited.

Habrobracon hebetor (Say, 1836) (Fig. 1a, b) is a gregarious, idiobiont, larval ectoparasitoid of pyralid moths (Lepidoptera) (Paust et al. 2006) and is well known for its use in biological pest control (Paust et al. 2006; Mbata and Shapiro-ilan 2010; Sanower et al. 2018). Dweck et al. (2008) provided the first morphological descriptions of the ovipositor of this species, with a strong focus on the terebra and its sensillar equipment. In the present study, however, we aim to describe thoroughly all the inherent cuticular elements of the ovipositor of *H. hebetor* in order further to discuss their structural, mechanical, and functional aspects. We have therefore combined scanning electron microscopic (SEM) and light-microscopic studies on both complete cuticular structures and histological serial sections. Serial sections of the terebra have been used to provide a 3D reconstruction that has helped us to understand its morphology especially with regard to all its functionally clustered inherent structures. Finally, we present a structural model of the braconid ovipositor and discuss its mode of function.

Materials and methods

Study animals

The *H. hebetor* (Fig. 1a, b) specimens used in this study originated from Sauter & Stepper GmbH (Ammerbuch, Germany), where they were bred on larvae of *Ephestia kuehniella* Zeller, 1879 (Lepidoptera: Pyralidae).

Sample preparation and light microscopy

For whole mount samples, female *H. hebetor* were killed in 70 % ethanol at 45 °C. The metasoma was cut off and macerated in 10% aqueous potassium hydroxide for up

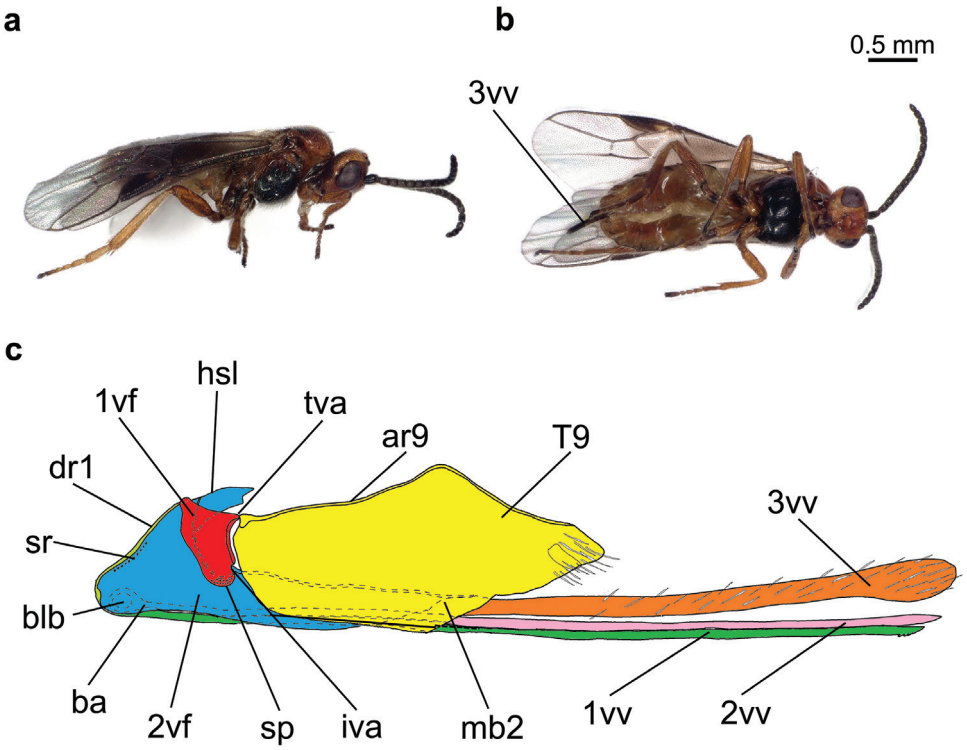

Figure 1. Habitus images of female *Habrobracon hebetor*: lateral (**a**) and ventral (**b**) aspect. Schematic drawing of the ovipositor of *H. hebetor* (lateral view) based on the light microscopic and SEM images (**c**). Abbreviations: 1vf = 1st valvifer; 1vv = 1st valvula; 2vf = 2nd valvifer; 2vv = 2nd valvula; 3vv = 3rd valvula; ar9 = anterior ridge of T9; ba = basal articulation; blb = bulb; dr1 = dorsal ramus of the 1st valvula; hsl = hook-shaped lobe of the 2nd valvifer; iva = intervalvifer articulation; mb2 = median bridge of 2nd valvifers; sr = sensillar row of the 2nd valvifer, sp = sensillar patch of the 2nd valvifer; T9 = female T9; tva = tergo-valvifer articulation.

to 24 h at room temperature to remove tissues, cleaned in distilled water on a mini-shaker, and dehydrated stepwise in ethanol. We then dissected the ovipositor out of the metasoma by using thin tungsten needles, mounted the specimen onto a microscope slide, and embedded it in Entellan® (Merck KGaA, Darmstadt, Deutschland).

For semithin serial sections, we anaesthetized female *H. hebetor* with carbon dioxide. The metasomas were removed and, in order to avoid autolysis, immediately submersed in a primary fixative containing 2.5% glutaraldehyde and 5% sucrose, buffered with 0.1 M cacodylate to pH 7.4. During this fixation, the samples were held in an ice bath at approximately 4 °C for 4 h. Samples were rinsed three times for 10 min in pre-chilled 0.1 M cacodylate buffer (pH 7.4) and post-fixed by using a solution of 1% osmium tetroxide in 0.1 M cacodylate buffer at 4 °C for 4 h. After being further rinsed in the same buffer, the samples were dehydrated through a graded series of ethanol with steps of 30% for 15 min and 50% for 10 min at 4 °C, three times per step, and of 70%

for 10 min, three times at room temperature. The following steps were performed at room temperature. *En bloc* staining was conducted using a saturated solution of 70% ethanolic uranyl acetate for 12 h on a rotatory shaker. Afterwards, dehydration was continued in 5% steps, three times for 10 min each. The fully dehydrated samples were washed in 100% propylene oxide twice for 1 h , and subsequently infiltrated in Spurr low-viscosity embedding resin (Polysciences Inc., Warrington, PA, USA) via a propylene oxide:resin mixture at ratios of 1:1, 1:3, and 1:7 for 1 h per step and then in pure resin for 17 h on a rotatory shaker. As a last incubation step, the samples were placed in fresh pure resin, embedded in silicon molds, and polymerized at 70 °C for 8 h.

Semithin sections of 600 nm were cut perpendicularly to the terebra of *H. hebetor* by using an ultramicrotome Leica Ultracut UTC (Leica Microsystems GmbH, Wetzlar, Germany) equipped with a diamond knife (45° knife angle; DuPont Instruments, Wilmington, DE, USA); a series was obtained with 1920 sections. Semithin sections were then mounted on a microscopic slide by using a 'Perfect Loop for Light Microscopy' (Electron Microscopy Sciences, Hatfield, PA, USA), stained with Stevenel's blue (del Cerro et al. 1980) for 40 min at 60 °C, and subsequently washed in distilled water twice for 5 min each. After being dried, the stained sections were embedded in 'Xylolfreies Eindeckmittel' (Engelbrecht Medizin- und Labortechnik GmbH, Edermüde, Germany).

The image stack for the 3D reconstruction was generated using a Zeiss Axioplan (Carl Zeiss Microscopy GmbH, Jena, Deutschland) light microscope, equipped with a Nikon D7100 single-lens reflex digital camera (Nikon K.K., Tokio, Japan) and Helicon Remote software version 3.6.2.w (Helicon Soft Ltd, Kharkiv, Ukraine). Flawed images (missing or folded structures and staining problems) were replaced by a copy of the previous or the following image (this was the case for fewer than 3% of the images) for reconstruction purposes. Adobe Photoshop Lightroom version 6.0 (Adobe Systems, San José, CA, USA) was used for initial image processing (white balancing, color contrasting, black and white conversion), whereas Fiji (Schindelin et al. 2012; available online at https://imagej.net/Fiji) was employed for cropping, CLAHE filtering, and image stack calibration by using the plugin TrakEM2 (Cardona et al. 2012). A preliminary least square rigid alignment followed by an elastic alignment of the image stack was performed using the 'Elastic Stack Alignment' plugin (Saalfeld et al. 2012). The aligned image stack was then imported into Amira version 6.0 (FEI Company, Hillsboro, OR, USA). We pre-segmented the 1st and 2nd valvulae, the duct of the venom gland and the ligaments that connect the terebra and the 2nd valvifer in the software's segmentation editor by manually labeling approximately every 15th virtual slice along the terebra and every 4th virtual slice in the proximal bulbous region and assigned them to different 'materials'. The labels served as an input for automated segmentation by using the Biomedical Image Segmentation App Biomedisa (available online at https://biomedisa.de) (Lösel et al. 2020). The output of Biomedisa was then partially corrected manually in Amira, and a final surface model was generated.

Schematic drawings of the cross-sections of the terebra were generated in Inkscape version 0.92.4 (Inkscape Community; available online at http://www.inkscape.org/) based on the original light-microscopic images of the semithin sections.

For lateral and ventral habitus images, female wasps were imaged with a Keyence VHX-7000 Digital Microscope (Keyence Corporation, Osaka, Japan) using focus stacking.

Scanning electron microscopy (SEM)

For scanning electron microscopy (SEM), the specimens were air-dried in a desiccator with Silica gel blue (Carl Roth GmbH & Co. KG, Karlsruhe, Deutschland) for at least four days before being mounted with double-sided adhesive tabs onto stubs and sputter-coated with 19 nm pure gold by using an Emitech K550X (Quorum Technologies Ltd, West Sussex, UK). Images were taken with a scanning electron microscope of the type EVO LS 10 (Carl Zeiss Microscopy GmbH, Jena, Germany) and SmartSEM version V05.04.05.00 software (Carl Zeiss Microscopy GmbH, Jena Germany).

Results and discussion

As in all hymenopterans, the ovipositor of *H. hebetor* consists of three pairs of valvulae, two pairs of valvifers, and the female T9 (Fig. 1c).

Overall structure of the terebra

The 1st and 2nd valvulae form the terebra and enclose the egg canal (cf. Figs 2c–g, 3; Suppl. material 1). The terebra of *H. hebetor* extends far beyond the posterior tip of the metasoma. They are interconnected by a tongue and groove-like system, called the olistheter (oth; Fig. 2a–h). The olistheter comprises two longitudinal ridges that are called the rhachises (rh; Figs 2a, 5c, d) on both sides at the ventral surface of the 2nd valvula and that fit into corresponding T-shaped grooves termed the aulaxes (au; Figs 2a, 4b, f, h)

Figure 2. (next page) Cross sections through the terebra of *Habrobracon hebetor* (from proximal to distal); schematic drawings of the 1st and 2nd valvula (**a–i**) based on the light microscopic images of the presented semithin sections (**a'–i'** 600 nm; stained with Stevenel's blue). The drawings are of the same size ratio. The 2nd valvulae possesses, in the proximal region, two lumina that merge into one in the most distal region (**h–i**). The bulbs (**b**) and the valvilli (**g**) are visible. The orange lines (in **e, f**) mark the position of the distally pointing ctenoid structures on the dorsal surfaces of the 1st valvulae, which are in close contact with the ventral surface of the 2nd valvula. The genital membrane connects the dorsal margins of the 2nd valvifers (**b'–h'**) **c** fine cuticular structures arise from the dorsal and ventral parts of the 2nd valvula and define the lumina of the bulbs (arrow) **h l** olistheter-like interlocking system connecting the medial surfaces of the apices of the paired 1st valvulae (arrow). Final segmented 3D reconstruction based on a semithin section series (600 nm thickness) **a*–i*** position of each single section marked on the final 3D reconstruction of the terebra. Abbreviations: 1vv = 1st valvula; 2vv = 2nd valvula; 3vv = 3rd valvula; au = aulax; blb = bulb; cr = longitudinal crack of 2nd valvula; ec = egg canal; fl1 = longitudinal flap of the 1st valvula; gm = genital membrane; igs = internal guiding structure; l1 = lumen of 1st valvula; l2 = lumen of 2nd valvula; lb = lumen of the bulb; lg = ligament; oth = olistheter; rh = rhachis; vd = duct of the venom gland; vl = valvillus.

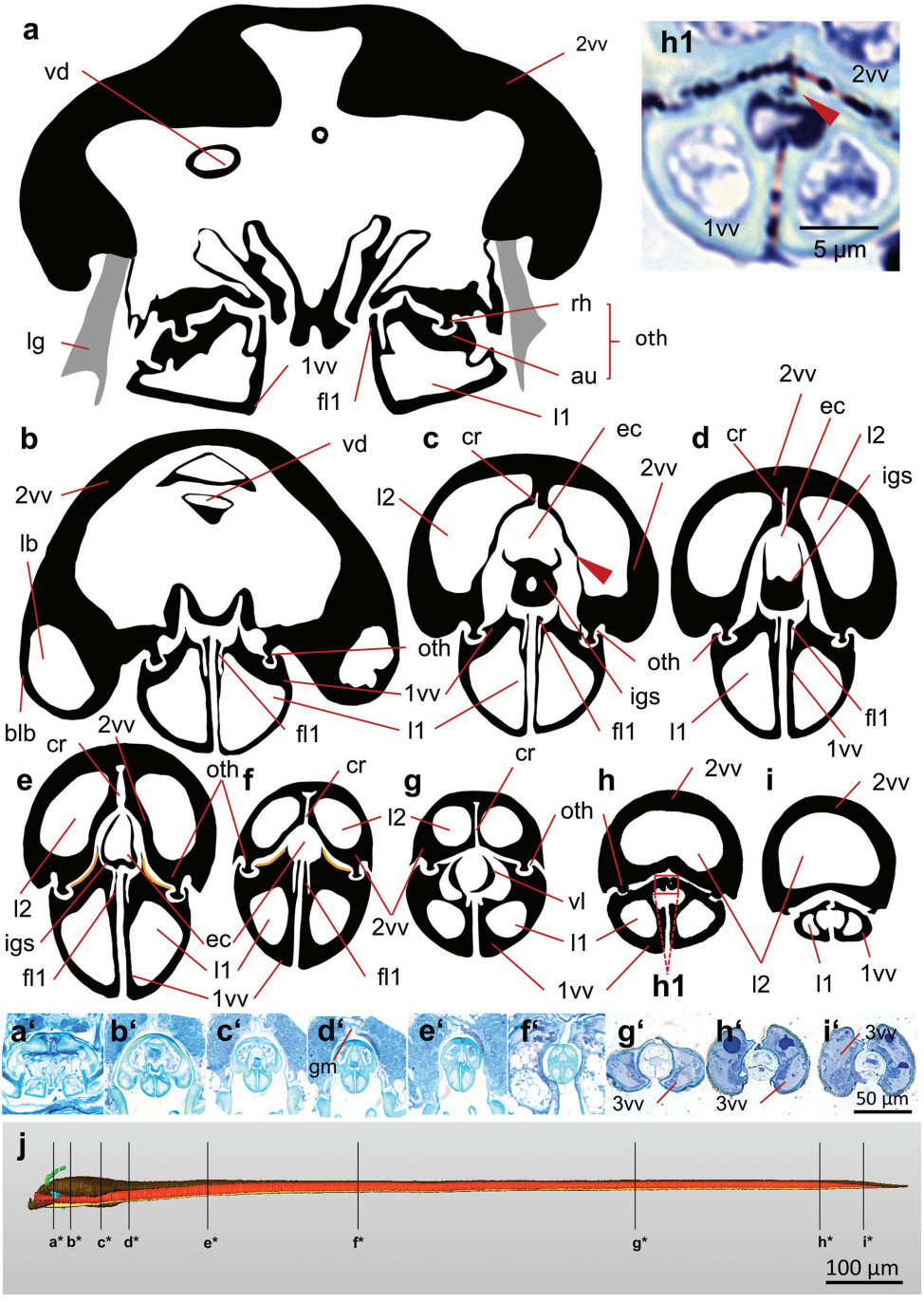
a
vd
2vv
lg
rh
au
oth
1vv
fl1
l1
h1
2vv
1vv
5 µm
b
vd
2vv
lb
blb
cr
2vv
oth
1vv
fl1
l1
c
cr
ec
2vv
l2
oth
igs
fl1
d
cr
2vv
ec
l2
igs
l1
fl1
1vv
e
oth
l2
igs
fl1
f
cr
ec
l1
1vv
fl1
g
cr
l2
oth
2vv
vl
l1
1vv
h
2vv
h1
i
2vv
l2
l1
1vv
a‘
b‘
c‘
d‘
gm
e‘
f‘
g‘
3vv
h‘
3vv
i‘
3vv
50 µm
j
a* b* c* d* e* f* g* h* i*
100 µm

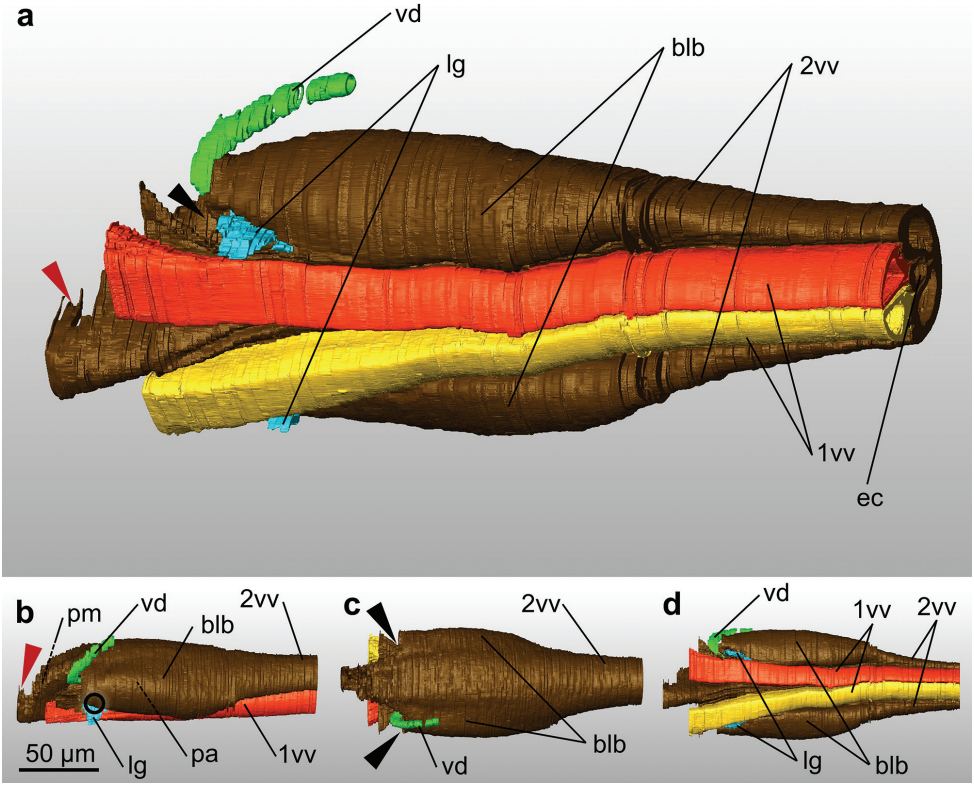

Figure 3. 3D reconstruction of the basal part of the terebra of *Habrobracon hebetor* composed of the 2nd valvulae and the paired 1st valvulae, based on a semithin section series (600 nm thickness **a** lateroventral aspect **b** lateral aspect **c** dorsal aspect **d** ventral aspect). The duct of the venom gland enters dorsoproximally on the left side only. The two ligaments connect the 2nd valvula to the anterior parts of the 2nd valvifers (not visible in these images). The black circle (**b**) indicates the rotation axis of the basal articulation. The lines of the processus articularis and processus musculares (**b**) point to their presumed position according to the results of van Meer et al. (2020). The peak-like structure at the anterior end of the 2nd valvula (red arrow in **a, b**) is part of the processus musculares. There are two openings (black arrows in **a, c**) at the proximal side of the bulbs. The duct of the venom gland enters on the left side only. Abbreviations: 1vv = 1st valvula; 2vv = 2nd valvula; blb = bulb; ec = egg canal; lg = ligament; pa = processus articularis; pm = processus musculares; vd = duct of the venom gland.

along the dorsal surface of each of the 1st valvulae. This system allows the 1st valvulae to slide longitudinally relative to each other when actuated by the corresponding operating muscles (Oeser 1961; Quicke et al. 1994). Distally pointing scale-like structures are found on both the olistheter elements and might reduce the friction forces by reducing the contact surface between the 1st valvulae and the 2nd valvula (sc; Fig. 4f) (Rahman et al. 1998).

In *H. hebetor*, the cross sections of the terebra differ notably along its length (Fig. 2a–i). A common oviduct enters the proximal bulbous part of the terebra (Bender

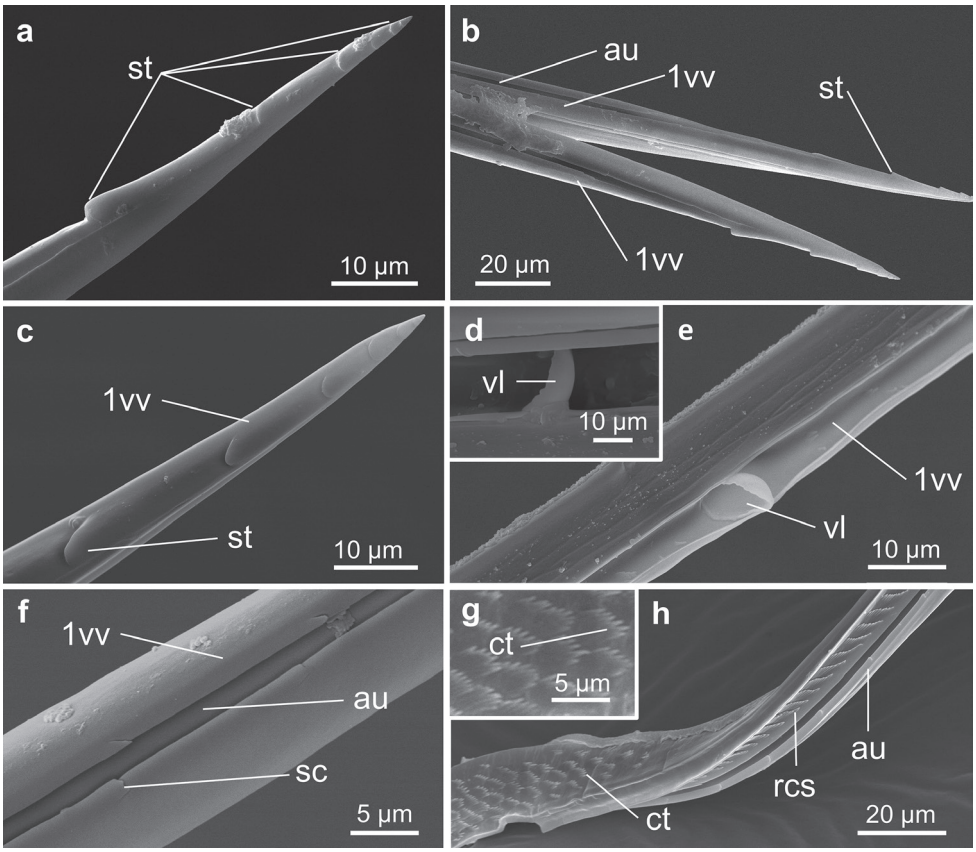

Figure 4. SEM images of the 1st valvulae of *Habrobracon hebetor* **a–c** apex of 1st valvula with sawteeth (**a** lateral aspect **b–c** dorsal aspect). The aulaces are visible (**b**) **d–e** valvillus of 1st valvula (distal is right) **f** distally oriented scale-like structures on the lateral walls of the aulax **g** leaf-like ctenidia on the medial side of 1st valvula **h** 1st valvula with distally oriented ctenoid structures on its dorsal side (contact surface with the 2nd valvula) and ctenidia on its medial side (contact surface with the opposing 1st valvula building the egg canal in the distal part of the terebra). Abbreviations: 1vv = 1st valvula; au = aulax; ct = ctenidium; rcs = row of ctenoid structures; sc = scales; st = sawtooth; vl = valvillus.

1943; Pampel 1914), where it ends at the base of the egg canal (Quicke 1997). Distally, the egg canal is largely defined by the 1st valvulae, but with the dorsal side being formed by the 2nd valvula. The diameter of the terebra decreases from proximal to distal, whereas the diameter of the egg canal remains constant for a long distance from proximal until the valvillus (see subsection '1st valvulae').

1st valvulae

The paired 1st valvulae of *H. hebetor* form the ventral half of the terebra (1vv; Figs 1c, 2a–i, 3, 7a). The proximal end of each 1st valvula is continuous with its dorsal ramus

(dr1; Figs 1c, 7c, h), which is fused with the anterodorsal corner of the 1st valvifer (Figs 7a, c, e, 8).

At their apices, the 1st valvulae of *H. hebetor* possess several sawteeth, which decrease in size apically (st; Fig. 4a, b, c) (cf. Dweck et al. 2008). They probably serve to penetrate the substrate and the host's skin and tissue. Distally pointing ctenoid structures (rcs; Fig. 4h) arranged in rows can be found on the dorsal surfaces of the 1st valvulae, which are in close contact with the ventral surface of the 2nd valvula (orange line; Fig. 2e, f). These ctenoid structures potentially reduce friction forces by minimizing the contact surface between the 1st and the 2nd valvula. The aulaces do not extend all the way to the apex of the 1st valvulae but end just before the lateral sawteeth occur (au; Fig. 4b). Both 1st valvulae are separated for the most of their length. However, mediodorsally at their very apex, the two 1st valvulae become interlocked dorsally by a mechanism similar to that of the olistheter (Fig. 2h1; also see fig. 4a of Dweck et al. 2008). Such a mechanism has previously been observed in other braconids (*Zaglyptogastra* (Quicke 1991), *Aleiodes*, *Ligulibracon* and *Odontobracon* (Quicke et al. 1994), and *D. longicaudata* (van Meer et al. 2020)) and is suggested to be an adaptation to the injection of venom into the host while laying the egg externally (Dweck et al. 2008). In addition, this mechanism might also increase the stability of the apex of the terebra when the host cuticle is pierced (Quicke 2015).

A single valvillus situated on the inner surface of each 1st valvulae protrudes inside the egg canal (vl; Figs 2g, 4d, e; cf. Dweck et al. 2008). The valvillus is a bilaterally concave structure lying in the distal third of the terebra and occupies the whole diameter of the egg canal. Valvilli can be found in the Ichneumonoidea and in various families of the Apocrita (Snodgrass 1933; Quicke et al. 1992; Rahman et al. 1998). They are postulated to serve as a stop and release mechanism for the egg by maintaining the egg in position within the terebra and blocking the egg canal in Ichneumonoidea (Rogers 1972; Rahman et al. 1998; Boring et al. 2009), or for venom pumping in Apocrita (Quicke et al. 1992). However, in the ectoparasitoid *H. hebetor*, the eggs are observed to advance and even partially emerge ventrally at the base of the terebra, i.e. in between the 1st valvulae and near the genital opening (Prozell et al. 2006; Wührer et al. 2009, see also Shaw 2017). Further distally, the valvilli seem to divert the egg ventrally between the 1st valvulae and to press it out completely, since the egg does not emerge at the tip of the terebra but rather ventrally in between the 1st valvulae approximately at the region at which the valvilli are located (Prozell et al. 2006; Wührer et al. 2009). We therefore suggest that the valvilli guide the relatively large egg ventrally out in between the 1st valvulae. The latter are capable of being widely spread in this region because of the olistheter mechanism (Shaw 2017). In cross sections further apically to the valvilli, an egg canal is rarely visible or is absent (Fig. 2h, i), which suggests that at that point the egg has already left the terebra. In addition, the apical interlocking in between the two 1st valvulae (red arrow; Fig. 2h1), which is similar to that of the olistheter, prevents the canal from expanding at the very apex. Proximal to the valvillus, the walls of the egg canal carry leaf-like ctenidia (ct; Fig. 4g, h), which are arranged in rows and are directed towards the distal end of the terebra. These rows of ctenidia point distally in

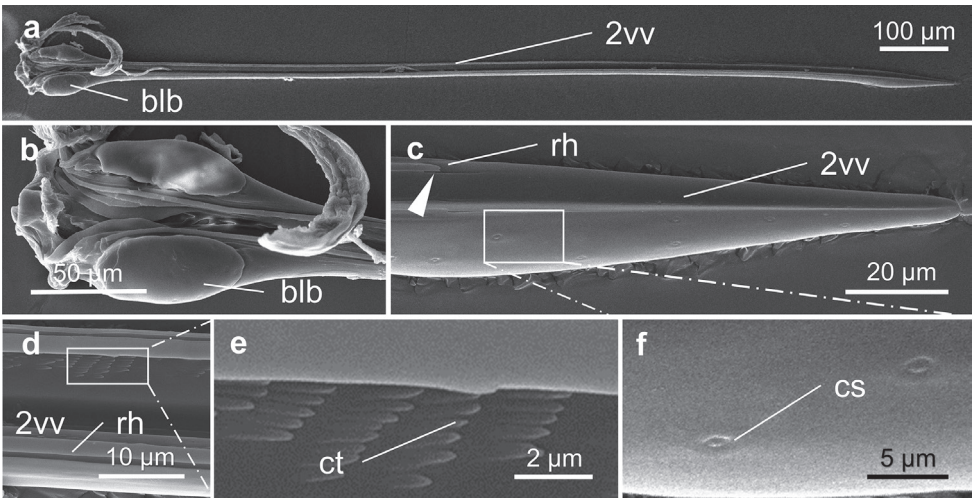

Figure 5. SEM images of the 2nd valvula of *Habrobracon hebetor* **a** overview of the 2nd valvula (ventral aspect with the interlocked 1st valvulae removed) **b** proximal part of 2nd valvula featuring the bulbs **c** apex of 2nd valvula with the ending of the rhachises (arrow) and campaniform sensillae (medioventral aspect) **d–e** middle part of the 2nd valvula showing the rhachises and distally oriented ctenidia **f** sensilla at the apex of the 2nd valvula (detail image of **c**). Abbreviations: 2vv = 2nd valvula; blb = bulb; cs = campaniform sensilla; ct = ctenidia; rh = rhachis.

the direction of egg movement and presumably prevent the regression of the egg during the oviposition process (Austin and Browning 1981). Setiform structures (= subctenidial setae *sensu* Rahman et al. 1998) are also found at the inner walls of the 1st valvulae lying distally to the valvilli. They are arranged in distinct rows.

Each 1st valvula contains a lumen (l1, Fig. 2a–i) whose cuticular walls differ along its length. Proximally, the cuticle is thin but becomes thicker towards the middle and diminishes again apical to the valvillus (Fig. 2a–i). In cross section, the shape of the 1st valvula differs between the basal region and the rest of the terebra. In the basal part, it is triangular in shape (1vv; Fig. 2a), whereas further distally, it appears more oval (1vv; Fig. 2b–i). A longitudinal flap extends along the mediodorsal edge for most of the length of the 1st valvulae and is clearly recognizable in cross sections (fl1; Fig. 2a–f). This flap is highly prominent in the proximal part of the terebra but vanishes further apically (fl1; Fig. 2g–i). It might seal the egg canal to prevent the leaking of venom, since the pressure of the venom has been suggested to squeeze the two flaps together and therefore to seal the gap (Quicke et al. 1994; Shaw 2017). It has been observed in almost all the examined braconid species (Quicke and van Achterberg 1990; Quicke et al. 1994).

2nd valvula

In *H. hebetor*, the 2nd valvula (2vv; Figs 1c, 2a–i, 3, 5a, 7a) form the dorsal half of the terebra, and its proximal bulbous end (blb; Figs 1c, 2b, 3, 5b, 7e, h; called the

bulbs in the following) is connected with the 2nd valvifer via the basal articulation (ba; Figs 1c, 7h).

The apex of the 2nd valvula is not serrated but is slightly enlarged before it narrows towards the tip (Figs 5a, c, 7a). In contrast to many ichneumonid and other braconid species (cf. Boring et al. 2009; Shah et al. 2012; Eggs et al. 2018), the 2nd valvula of *H. hebetor* does not feature a prominent apical notch. Campaniform sensilla can be found in this area (cs; Fig. 5f) (for a discussion of the sensillary equipment of the terebra of *H. hebetor*, see Dweck et al. 2008). Similar to the aulaces on the 1st valvulae, the rhachises (rh; Fig. 5c, d) do not extend all the way to the apex but end at about the same distance away from the apex as seen for the aulaces (arrow; Fig. 5c). The apical half of the ventral side of the 2nd valvula forms the dorsal wall of the egg canal and is, similar to the 1st valvulae, covered by rows of ctenidia directed distally (ct; Fig. 5e). As previously discussed for the 1st valvulae, these structures might prevent the regression of the egg during oviposition (cf. Rahman et al. 1998). Medioproximally, the bulbs feature ligaments (lg; Figs 2a, 3a, b, d) that connect the 2nd valvula with the anterior section of the 2nd valvifer. The ligament marks the region at which parts of the 2nd valvifer merge into the anterior part of the 2nd valvula. The bulbs also contain a lumen (lb; Fig. 2b). The proximal end of the 2nd valvula bears the processus articularis (pa; Figs 3b, 7h) laterally and the processus musculares (pm; Figs 3b, 7h) at the anterior peak-like structure of the 2nd valvula (red arrow; Fig. 3a, b). However, the medial 2nd valvifer-2nd valvula muscle (M-2vfl-2vlv) that might stabilize the 2nd valvifer and that was newly described in the braconid *D. longicaudata* by Meer et al. (2020) was absent in our serial sections. There are two openings (black arrows; Fig. 3a, c) at the proximal side of the bulbs. The duct of the venom gland enters the dorsoproximal area of the bulbs on the left side only (vd; Figs 2a, b, 3, Suppl. material 2) (cf. Bender 1943, who investigated the anatomy and histology of the female reproductive organs of the closely related *Habrobracon juglandis* (Ashmead, 1889)). Further distally, the closed duct of the venom gland seems to disappear and to merge with the egg canal formed by the valvulae (Suppl. material 2). In this area, the venom presumably flows into the egg channel that is formed by both the 1st and 2nd valvulae with the longitudinal flaps of the 1st valvulae acting as a seal (fl1; Fig. 2a–f).

Proximally, the 2nd valvula features a distinct longitudinal crack at the ventral side along the middle, which is clearly visible in cross-section (cr; Fig. 2c–g), presumably indicating the paired origin of the 2nd valvulae. At the basal part of the 2nd valvula, fine cuticular structures (arrow; Fig. 2c) arise from it dorsal and ventral parts and define the two lumina (l2; Fig. 2c–g) that run almost the entire length of the 2nd valvula and that fuse at the apex (Fig. 2h, i). Proximally, the ventral part of the 2nd valvula gradually changes shape and forms a U-shaped structure that extends distally into the egg canal (Suppl. material 2). This internal structure (igs; Fig. 2c–e) presumably helps in guiding the egg by forming a temporary egg canal. Without this internal guiding structure, the diameter of the egg canal would be large in this proximal region; this might lead to a lowered internal pressure and thus to problems when the egg is pushed further distally.

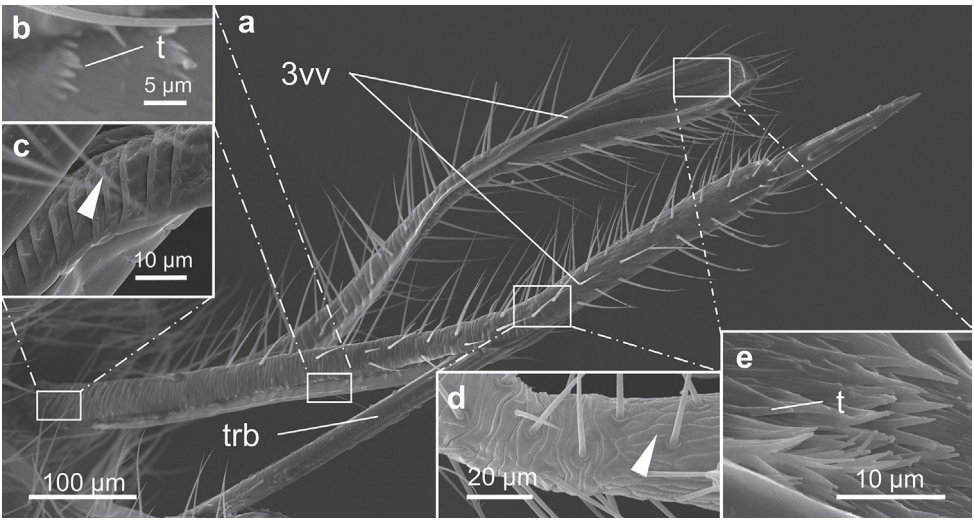

Figure 6. SEM images of 3rd valvulae of *Habrobracon hebetor* **a** the terebra is partially embraced by the 3rd valvulae **b** inner proximal surface of the 3rd valvulae with fine trichomes distally **c** outer surface of the 3rd valvulae, proximally exhibiting annulation caused by fine transverse furrows (arrow) **d** outer surface of the 3rd valvulae at the transition zone (arrow) between the distal longitudinal ridge to the proximal vertically folded surface at the region in which the 3rd valvulae expand **e** inner surface of the apex of a 3rd valvula covered by trichomes. Abbreviations: 3vv = 3rd valvula; trb = terebra; t = trichome.

3rd valvulae

The paired 3rd valvulae of *H. hebetor* originate at the distal end of the 2nd valvifers and extend far beyond the posterior tip of the metasoma towards the tip of the terebra (Figs 1b,c, 7a, e). Each is U-shaped in cross-section (3vv; Figs 2g'–i', 6a) and they completely ensheath and protect the terebra in the resting position (3vv, trb; Figs 2g'–i', 6a) (cf. Bender 1943; Dweck et al. 2008). The distal third of the 3rd valvulae is enlarged (Figs 6a, 7a), and their lateral surfaces differ over the course of their length: proximally, the 3rd valvulae are annulated by fine transverse furrows (arrow; Fig. 6c; cf. Vilhelmsen 2003; Eggs et al. 2018), whereas the enlarged distal part lacks these structures (arrow; Fig. 6d). Trichomes, which Dweck et al. (2008) have described as trichoid sensilla, cover most of the external surface of the 3rd valvulae (Fig. 6a). The density of the trichomes varies along the length of the 3rd valvulae and is highest at the apex (Fig. 6a).

The inner surface of the 3rd valvulae facing the terebra is densely covered by trichomes (t; Fig. 6b, e), particularly at the distal enlarged part (Fig. 6a, e). These structures might be involved in cleaning the terebra sensilla between oviposition episodes (Quicke et al. 1999; Vilhelmsen 2003). Observations have shown that the 3rd valvulae also play a role in stabilizing the terebra during oviposition (Prozell et al. 2006; Wührer et al. 2009; Vilhelmsen 2003; Cerkvenik et al. 2017; Eggs et al. 2018; van Meer et al. 2020).

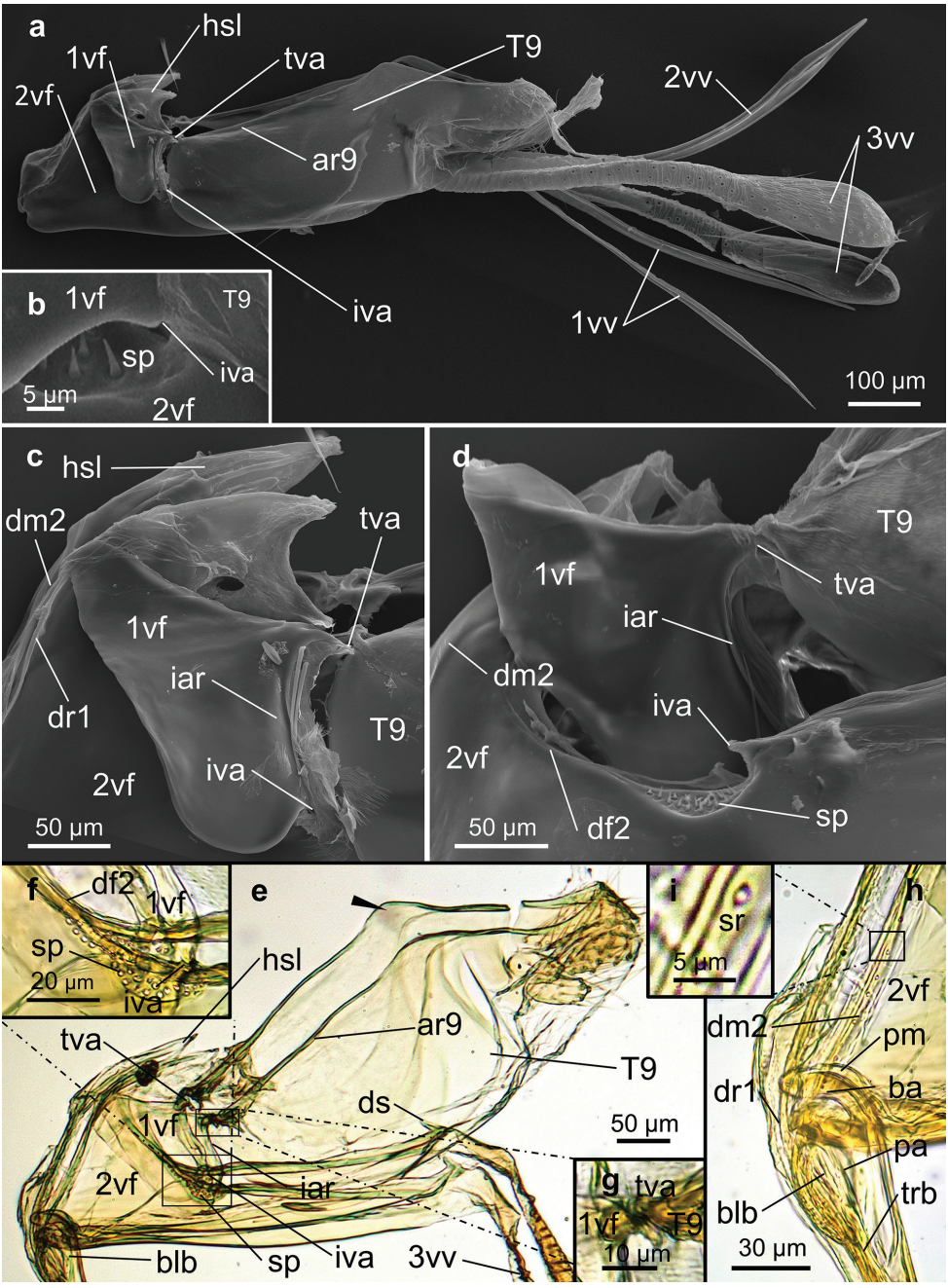
a
hsl
1vf
tva
T9
2vf
2vv
3vv
ar9
iva
1vv
100 µm
b 1vf
T9
sp
iva
5 µm
2vf
c hsl
dm2
tva
1vf
iar
dr1
T9
2vf
iva
50 µm
d
T9
1vf
tva
iar
dm2
iva
2vf
50 µm
df2
sp
f df2
1vf
sp
20 µm
iva
e
hsl
ar9
tva
T9
ds
1vf
50 µm
2vf
iar
blb
sp
iva
3vv
i
sr
5 µm
h
2vf
dm2
pm
dr1
ba
pa
trb
blb
30 µm
g tva
1vf
T9
10 µm

1st valvifer

In lateral view, the paired 1st valvifers of *H. hebetor* have a compact triangular shape with rounded edges (1vf; Figs 1c, 7a, c–e, 8). The intervalvifer articulation (iva; Figs 1c, 7a, c–f), a rotational joint, is located at the rounded posteroventral side and connects the 1st valvifer to the 2nd valvifer. The ventral edge of the 1st valvifer is placed laterally of the 2nd valvifer and seems to be in contact with a sensillar patch (sp; Figs 1c, 7b, d–f) that extends dorsally at the anterior beginning of the the dorsal flange of the 2nd valvifer (df2; Fig. 7d, f). The tergo-valvifer articulation (tva; Fig. 7a, c–e, g) connects the 1st valvifer to the female T9. A ridge, called the interarticular ridge of the 1st valvifer (iar; Figs 1c, 7c–e, 8), extends in between the two articulations. This ridge might mechanically stabilize the 1st valvifer and prevent it from extensive deformation. At its anterodorsal corner (arrow; Fig. 8), the 1st valvifer is fused with the dorsal ramus of the 1st valvula (dr1; Figs 1c, 7c, h, 8), which is continuous with the 1st valvula.

2nd valvifer

The paired 2nd valvifers of *H. hebetor* are elongated in the longitudinal axis (2vf; Figs 1c, 7a, e). The anteromedial socket-like part of the 2nd valvifer is connected to the laterally placed bulbs of the 2nd valvula (blb; Figs 1c, 3, 7e, h) via the ball-and-socket-like basal articulation (ba; Figs 1c, 7h). The posterior ends of both the 2nd valvifers are connected to the 3rd valvulae (3vv; Figs 1c, 7a, e). At their posterodorsal ends, the two 2nd valvifers are connected by a median bridge (mb2; suggested position indicated in Fig. 1c). A massive dorsal spike (ds; Fig. 7e), a structure that has not as yet been described in other parasitoid wasps, is present at the posterior end of the 2nd valvifer and potentially serves as an apodeme. In addition, a flexible cuticular area, a conjunctiva called the genital membrane (gm; Fig. 2d'), connects the ventral margins of the 2nd valvifers arching above the 2nd valvula.

Figure 7. (previous page) SEM (**a–d**) and light microscopic (**e–i**) images of the ovipositor of *Habrobracon hebetor* **a** overview of the ovipositor (lateral aspect; visible pore-like structures are presumably artefacts of detached trichomes) **c** 1st valvifer exhibiting the interarticular ridge and the hook-shaped lobe of the 2nd valvifer. The 1st valvifer is continuous with the dorsal rami of the 1st valvula and is articulated with the 2nd valvifer and the female T9 via the intervalvifer articulation and the tergo-valvifer articulation, respectively **d** sensillar patch of the 2nd valvifer (made visible by partly removal of the 1st valvifer) **b, f** sensillar patch of the 2nd valvifer **e** overview of the 2nd valvifer and female T9. The arrow shows the dorsal hump of the T9 **g** tergo-valfiver articulation between the 1st valvifer and female T9 **h** detail image of e. The laterally placed bulbs of the most proximal part of the 2nd valvula are articulated with the paired 2nd valvifers via the basal articulation **i** sensilla in a row at the dorsal margin of the 2nd valvifer. Abbreviations: 1vf =1st valvifer; 1vv = 1st valvula; 2vf = 2nd valvifer; 2vv = 2nd valvula; 3vv = 3rd valvula; ar9 = anterior ridge of T9; ba = basal articulation; blb = bulb; df2 = dorsal flange of 2nd valvifer; dm2 = dorsal margin of the 2nd valvifer; dr1 = dorsal ramus of the 1st valvula; ds = dorsal spike of the 2nd valvifer; hsl = hook-shaped lobe of the 2nd valvifer; iar = interarticular ridge of the 1st valvifer; iva = intervalvifer articulation; sp = sensillar patch of the 2nd valvifer; sr = sensillar row of the 2nd valvifer; pa = processus articularis; pm = processus musculares; T9 = female T9; trb = terebra; tva = tergo-valvifer articulation.

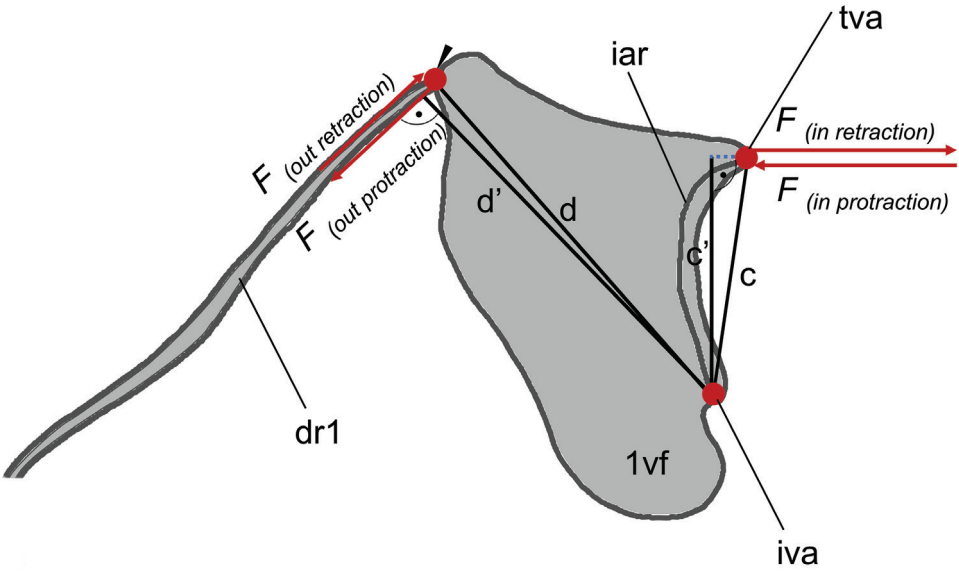

Figure 8. Functional lever model of 1st valvifer with both articulations and the beginning of the dorsal ramus of the 1st valvula (arrow) with the intervalvifer articulation acting as pivot point. c = anatomical inlever ; c' = effective (= mechanical) inlever; d = anatomic outlever; d` = effective (= mechanical) outlever; $F_{(\text{in protraction})}$, $F_{(\text{in retraction})}$ = Force input at the 1st valvifer; $F_{(\text{out protraction})}$, $F_{(\text{out retraction})}$ = Force output at the 1st valvifer that is transferred to the dorsal ramus of the 1st valvula. $c' \cdot F_{(in)} = d' \cdot F_{(out)}$. Abbreviations: 1vf = 1st valvifer; dr1 = dorsal ramus of the 1st valvula; iar = interarticular ridge of the 1st valvifer; iva = intervalvifer articulationtva = tergo-valvifer articulation.

At its anterodorsal corner, the 2nd valvifer extends upwards in a hook-shaped lobe (hsl; Fig. 7a, c, e; *sensu* Snodgrass 1933), and features the elongated anterodorsal ridge of the 2nd valvifer, the so called dorsal margin of the 2nd valvifer (dm2; Fig. 7c, d, h). The dorsal projection of the 2nd valvifer, a tongue-like structure situated on the dorsal margin of the 2nd valvifer, is continuous with the olistheter. The corresponding groove is located on the dorsal side of the dorsal ramus of the 1st valvula (dr1; Fig. 7c, h; cf. fig. 4h1 of Eggs et al. 2018) and enables its back and forth movement. This hook-shaped lobe might guide and stabilize the 1st valvifer during its posterior pivoting but might also allow for a larger arc of movement of the 1st valvifer and therefore a greater retraction distance of the 1st valvulae (cf. Eggs et al. 2018).

Two main ridges are found on the 2nd valvifer, i.e. (1) the dorsal flange of the 2nd valvifer (df2; Fig. 7d, f), which expands from the sensillar patch in the direction of the hook-shaped lobe and posteriorly from the sensillar patch to the origin of the 3rd valvulae (Fig. 7e), and (2) the dorsal margin of the 2nd valvifer (dm2; Fig. 7c, d, h). The two cuticular ridges might have a stabilizing function to prevent deformation. The 2nd valvifer of *H. hebetor* does not feature a basal line (e.g. in contrast to the ichneumonid *Venturia canescens* (Gravenhorst, 1829), see fig. 4e of Eggs et al. 2018), a ridge that extends from the pars articularis to the dorsal flange of the 2nd valvifer.

Clusters of sensillae ("styloconic sensillae" according to Dweck et al. 2008) occur in two regions. The first cluster, called the sensillar patch (sp; Figs 1c, 7b, d–f), is situated ventrally of the intervalvifer articulation and is covered by the 1st valvifer laterally. The second cluster occurs at the dorsal margin of the 2nd valvifer (sr; Figs 1c, 7h, i). These sensilla are arranged in a row and are in contact with the dorsal ramus of the 1st valvula. The two sensilla clusters presumably monitor the pro- and retraction movements of the 1st valvifers and the attached 1st valvulae, respectively. The density of sensilla in the patch is much higher than that on the dorsal margin of the 2nd valvifer.

Female T9

The female T9 is unpaired and elongated (T9; Figs 1c, 7a, c, d, e). At its anterodorsal corner, it is connected to the 1st valvifer via the tergo-valvifer articulation (tva; Figs 1c, 7a, c–e, g). Dorsally, it features the anterior ridge almost throughout its length (ar9; Fig. 7e), and posteriorly, it bears a hump-shaped structure (arrow; Fig. 7e). The female T9 mostly lies inside the abdomen, and only the posterolateral part that faces the outside is covered with hairs.

Mode of function of the ovipositor

Functional models of the actuation and movement mechanisms based on thorough analyses of the musculoskeletal system of an ichneumonid and a braconid wasp have recently been described (Eggs et al. 2020, van Meer et al. 2020) and are summarized in the following. Although, in our study, we have not considered the muscles of the system, we have basically found the same arrangement of cuticular elements in the ovipositor system of *H. hebetor* as described in both of the above-mentioned studies. Hence, we assume analogous functional morphological conditions, although we point out any possible *H. hebetor*-specific modifications.

The ovipositor movements are mainly actuated by two pairs of antagonistically working muscles (further described below), i.e. (1) the depression (i.e. downward rotation to the active position) and elevation (i.e. upward rotation back to the resting position) of the terebra, and (2) the pro- and retraction of the 1st valvulae. Smaller muscles, i.e. the 1st valvifer-genital membrane muscle or the posterior T9-2nd valvifer muscle, might predominantly serve to stabilize the ovipositor system during oviposition.

(1) Depression and elevation of the terebra: The basal articulation is composed of the processus articularis (pa; Figs 3b, 7h) at the 2nd valvulae and the pars articularis at the 2nd valvifer. The pars articularis is a small area of anteroventral corners of the 2nd valvifer, whereas the processus articularis is the respective structure of the bulb. The posterior 2nd valvifer-2nd valvula muscle depresses the terebra, i.e. rotates it downwards to the active position from its resting position between the paired 3rd valvulae. The tendon of this muscle inserts at the processus musculares (pm; Figs 3b, 7h), which is situated at the peak-like posterior part of the 2nd valvula (arrow; Fig. 3a, b) and thus

increases the moment arm. However, the moment arm most probably changes over the range of motion of the terebra. In *H. hebetor*, we assume that the virtual line that can be drawn perpendicularly to the length axis of the terebra through the ligaments (lg; Figs 2a, 3a, b, d) lying anterolaterally on the bulbs (blb; Figs 2b, 5a, b, 7e, h) most likely forms the rotation axis (= joint axis, pivot point or fulcrum; black circle; Fig. 3b), since the ligaments form the connections of the 2nd valvula with the anterior parts of the 2nd valvifers and can only stretch to a limited extent. Van Meer et al. (2020) postulate that, in the braconid *D. longicaudata*, the rotation axis lies directly anterior to the bulbs. In addition, these authors have observed that, during terebra depression (towards an active probing position), the lateral bulbs are pulled out of the socket-like anterior parts of the 2nd valvifers, which are pushed slightly apart. The ball-and-socket-like connection is therefore assumed mainly to stabilize the terebra in its resting position. The antagonistically acting anterior 2nd valvifer-2nd valvula muscle inserts at the processus musculares and elevates the terebra, i.e. rotates it back upwards towards the resting position.

(2) Pro- and retraction of the 1st valvulae: The 1st valvifer, 2nd valvifer, and the female T9 form a mechanical cluster of functionally interconnected elements (for detailed functional models see fig. 5 of Eggs et al. 2018 and fig. 8 of van Meer et al. 2020). The dorsal and the antagonistically acting ventral T9-2nd valvifer muscle change the relative position of the 2nd valvifer and the female T9. Both of these structures are connected with the 1st valvifer via the intervalvifer and the tergo-valvifer articulation (Fig. 7c), respectively. Moreover, both are rotational joints that allow rotation in the sagittal plane only. The 1st valvifer acts as a lever (Fig. 8) that transfers its movements to the dorsal ramus of the 1st valvula (dr1; Figs 7c, h, 8). Contraction of the dorsal T9-2nd valvifer muscle leads to an anterior rotation of the 1st valvifer around the intervalvifer articulation. The 1st valvifer acts as a lever that transfers these movements to the dorsal ramus of the 1st valvula, thus causing the 1st valvula to slide distally relative to the 2nd valvula, i.e. to protract. *Vice versa*, contraction of the antagonistic ventral T9-2nd valvifer muscle leads to a posterior rotation of the 1st valvifer, causing the 1st valvula to slide proximally to the 2nd valvula, i.e. to retract (Eggs et al. 2018; van Meer et al. 2020). The hook-shaped lobe of the 2nd valvifer (hsl; Fig. 7a, c, e) might allow a larger arc of movement of the 1st valvifer and therefore a larger retraction distance of the 1st valvulae. During the retraction of the 1st valvula, the dorsal ramus of the 1st valvula (dr1; Fig. 7c, h) can slide along the dorsal projection of the 2nd valvifer almost until the posterior end of the hook-shaped lobe (hsl; Fig. 7a, c, e).

In the context of the described movements, the 1st valvifer acts as a one-armed class 3 lever (force arm smaller than load arm). In our lever model (Fig. 8), we use the 2nd valvifer (2vf; Fig. 1c) as a frame of reference. However, in reality, all involved cuticular elements can move relative to each other. The anatomical inlever (c; Fig. 8) equals the distance between the intervalvifer articulation and the tergo-valvifer articulation (where the input force is applied; $F_{(\text{in protraction})}$, $F_{(\text{in retraction})}$; Fig. 8). The distance between the intervalvifer articulation and the beginning of the dorsal ramus of the 1st valvula at the anterodorsal end of the 1st valvifer equals the anatomical outlever (d; Fig. 8). The ratio of effective outlever (d'; Fig. 8) and the effective inlever (c'; Fig. 8) are indicative for the potential

maximum velocity, the mechanical deflection, and the amount of force transmission to the 1st valvula. An increase of the d':c' ratio results in an increase of the potential maximum velocity and mechanical deflection but entails a smaller force output ($F_{(\text{out protraction})}$, $F_{(\text{out retraction})}$; Fig. 8) of the 1st valvulae. In resting position, the anatomical in- and outlever are both very similar to their respective effective levers, thereby creating high torques at the intervalvifer articulation and ensuring an optimal force transmission when pro- or retracting the 1st valvulae. During oviposition, the left and the right 1st valvulae slide back and forth alternately at a high frequency. These valvula movements are crucial for drilling and precise egg laying (Vilhelmsen 2000; Cerkvenik et al. 2017; van Meer et al. 2020).

The shape of the 1st valvifer varies between the various hymenopteran superfamilies (Oeser 1961). Ichneumonoid species such as the braconid *H. hebetor* in the present study possess a 1st valvifer with a rounded compact shape (Snodgrass 1933; Eggs et al. 2018), in contrast to the elongated and bow-shaped 1st valvifers of members of the superfamily Chalcidoidea (Copland and King 1972a, 1972b, 1972c, 1973), the triangularly shaped 1st valvifers of *Apis mellifera* (Linnaeus, 1758) and other aculeate species (Snodgrass 1933; Oeser 1961; Matushkina 2011; Matushkina and Stetsun 2016; Stetsun and Matushkina 2020; Graf et al. 2021), and the highly diverse 1st valvifers of basal hymenopterans (e.g. the robust-appearing 1st valvifers of Tentredinidae (Snodgrass 1933; Vilhelmsen 2000) or the triangular 1st valvifers in some Xyelidae (Vilhelmsen 2000). The ecomorphological consequences of these morphological differences remain to be explored in future systematic comparative analyses with respect to the parasitization of other hosts in different substrates and habitats.

The two sensilla clusters found on the 2nd valvifer of *H. hebetor* (sp, sr; Fig. 7b, d–f, i). probably play an important role in monitoring the pro- and retraction of the 1st valvulae, since their accurate actuation is of major importance for successful egg deposition (van Meer et al. 2020). Unlike in *H. hebetor* or *V. canescens* (Eggs et al. 2018), the sensilla patch at the intervalvifer articulation of other parasitoid wasps can be extremely reduced, e.g. in Pteromalidae (Chalcidoidea) with only three single sensilla (Copland and King 1972b). The question remains as to whether both the density and number of sensilla are linked to the importance of the control of the movements involved in oviposition, and whether this correlates with the shape of the 1st valvifer.

Conclusion

All the cuticular elements of the ovipositor of *Habrobracon hebetor* play a crucial role for successful oviposition. The 2nd valvifer and the female T9 exhibit many muscle insertions, the 1st valvifer acts as a lever that transmits movements to the 1st valvulae, and the terebra serves as a device for precise venom injection, host assessment, and accurate egg laying. All the cuticular elements feature many distinct structures in addition to the microsculpture that is crucial for the performance of these tasks. Our work also has shown that a 3D reconstruction based on a histological section series preserves useful information about the exact morphology and position of inherent structures thereby enabling us to draw conclusions about their function. Future comparative examination of the inherent ovipositor

elements, their morphological structure, and the underlying mechanical and functional aspects has the potential to increase our understanding of a putative key feature in the evolution of parasitoid hymenopterans, a feature that probably has significantly impacted the evolutionary success of braconid wasps (more than 18,000 described (Quicke 2015) and about 43,000 estimated species (Jones et al. 2009)) and of parasitoid hymenopterans in general (115,000 described and 680,000 estimated species (Heraty 2009)).

Acknowledgements

We thank Paavo Bergmann for valuable hints regarding histological techniques, Monika Meinert for assistance with SEM, Verena Pietzsch and James H. Nebelsick with the Keyence digital microscope, Theresa Jones for linguistic corrections of the manuscript, and Lars Vilhelmsen and Donald L. J. Quicke for their useful comments.

This work was funded by the German Research Foundation (DFG) as part of the Transregional Collaborative Research Centre (SFB-TRR) 141 'Biological design and integrative structures' (project A03 'Inspired by plants and animals: actively actuated rod-shaped structures exhibiting adaptive stiffness and joint-free kinematics'). The article processing charge was covered by the DFG and the Open Access Publishing Fund of the University of Tübingen.

References

Alam SM (1953) The skeleto-muscular mechanism of *Stenobracon deesae* Cameron (Braconidae, Hymenoptera) – An ectoparasite of sugarcane and juar borers of India. Part II. Abdomen and internal anatomy. Aligarh Muslim University Publications (Zoology Series) 3: 1–75

Austin AD, Browning TO (1981) A mechanism for movement of eggs along insect ovipositors. International Journal of Insect Morphology and Embryology 10: 93–108. https://doi.org/10.1016/S0020-7322(81)80015-3

Barbosa DN, Vilhelmsen L, Azevedo CO (2021) Morphology of sting apparatus of Chrysidoidea (Hymenoptera, Aculeata). Arthropod Structure & Development 60: 100999. https://doi.org/10.1016/j.asd.2020.100999

Bender JC (1943) Anatomy and histology of the female reproductive organs of *Habrobracon juglandis* (Ashmead) (Hymenoptera, Braconidae). Annals of the Entomological Society of America 36: 537–545. https://doi.org/10.1093/aesa/36.3.537

Boring CA, Sharkey M, Nychka J (2009) Structure and functional morphology of the ovipositor of *Homolobus truncator* (Hymenoptera: Ichneumonoidea: Braconidae). Journal of Hymenoptera Research 18: 1–24.

Cardona A, Saalfeld S, Schindelin J, Arganda-Carreras I, Preibisch S, Longair M, Tomancak P, Hartenstein V, Douglas RJ (2012) TrakEM2 software for neural circuit reconstruction. PLoS ONE 7: e38011. https://doi.org/10.1371/journal.pone.0038011

Cerkvenik U, van de Straat B, Gussekloo SWs, van Leeuwen JL (2017) Mechanisms of ovipositor insertion and steering of a parasitic wasp. Proceedings of the National Academy of Sciences of the United States of America 114: E7822–E7831. https://doi.org/10.1073/pnas.1706162114

del Cerro M, Cogen J, del Cerro C (1980) Stevenel's blue: an excellent stain for optical microscopical study of plastic embedded tissues. Microscopica Acta 83: 117–121.

Copland MJW (1976) Female reproductive system of the Aphelinidae (Hymenoptera: Chalcidoidea). International Journal of Insect Morphology and Embryology 5: 151–166. https://doi.org/10.1016/0020-7322(76)90001-5

Copland MJW, King PE (1972a) The structure of the female reproductive system in the Eurytomidae (Chalcidoidea: Hymenoptera). Journal of Zoology 166: 185–212. https://doi.org/10.1111/j.1469-7998.1972.tb04085.x

Copland MJW, King PE (1972b) The structure of the female reproductive system in the Pteromalidae (Chalcidoidea: Hymenoptera). The Entomologist 105: 77–96.

Copland MJW, King PE (1972c) The structure of the female reproductive system in the Torymidae (Hymenoptera: Chalcidoidea). Transactions of the Royal Entomological Society of London 124: 191–212. https://doi.org/10.1111/j.1365-2311.1972.tb00363.x

Copland MJW, King PE (1973) The structure of the female reproductive system in the Agaonidae (Chalcidoidea, Hymenoptera). Journal of Entomology Series A, General Entomology 48: 25–35. https://doi.org/10.1111/j.1365-3032.1973.tb00029.x

Dweck HKM, Gadallah NS, Darwish E (2008) Structure and sensory equipment of the ovipositor of *Habrobracon hebetor* (Say) (Hymenoptera: Braconidae). Micron 39: 1255–1261. https://doi.org/10.1016/j.micron.2008.03.012

Eggs B, Birkhold AI, Röhrle O, Betz O (2018) Structure and function of the musculoskeletal ovipositor system of an ichneumonid wasp. BMC Zoology 3: 12. https://doi.org/10.1186/s40850-018-0037-2

Ernst AF, Mikó I, Deans AR (2013) Morphology and function of the ovipositor mechanism in Ceraphronoidea (Hymenoptera, Apocrita). Journal of Hymenoptera Research 33: 25–61. https://doi.org/10.3897/jhr.33.5204

Fergusson NDM (1988) A comparative study of the structures of phylogenetic importance of female genitalia of the Cynipoidea (Hymenoptera). Systematic Entomology 13: 13–30. https://doi.org/10.1111/j.1365-3113.1988.tb00225.x

Field SA, Austin AD (1994) Anatomy and mechanics of the telescopic ovipositor system of *Scelio latreille* (Hymenoptera: Scelionidae) and related genera. International Journal of Insect Morphology and Embryology 23: 135–158. https://doi.org/10.1016/0020-7322(94)90007-8

Frühauf E (1924) Legeapparat und Eiablage bei Gallwespen (Cynipidae). Zeitschrift für Wissenschaftliche Zoologie 121: 656–723.

Gauld I, Bolton B (Eds) (1988) The Hymenoptera. Oxford University Press, Oxford, 332 pp.

Graf S, Willsch M, Ohl M (2021) Comparative morphology of the musculature of the sting apparatus in *Ampulex compressa* (Hymenoptera, Ampulicidae) and *Sceliphron destillatorium* (Hymenoptera, Sphecidae). Deutsche Entomologische Zeitschrift 68: 21–32. https://doi.org/10.3897/dez.68.58217

Hanna AD (1934) The male and female genitalia and the biology of *Euchalcidia aryobori* Hanna (Hymenoptera, Chalcidinae). Transactions of the Royal Entomological Society of London 82: 107–136. https://doi.org/10.1111/j.1365-2311.1934.tb00030.x

Heraty J (2009) Parasitoid biodiversity and insect pest management. In: Foottit RG, Adler PH (Eds) Insect Biodiversity: Science and Society. Wiley-Blackwell, Oxford, 445–462. https://doi.org/10.1002/9781444308211.ch19

Hymenoptera Anatomy Consortium (2021) Hymenoptera Anatomy Ontology. [Accessed 12 January 2021]

Jones OR, Purvis A, Baumgart E, Quicke DLJ (2009) Using taxonomic revision data to estimate the geographic and taxonomic distribution of undescribed species richness in the Braconidae (Hymenoptera: Ichneumonoidea). Insect Conservation and Diversity 2: 204–212. https://doi.org/10.1111/j.1752-4598.2009.00057.x

King PE (1962) The muscular structure of the ovipositor and its mode of function in *Nasonia vitripennis* (Walker) (Hymenoptera: Pteromalidae). Proceedings of the Royal Entomological Society of London. Series A, General Entomology 37: 121–128. https://doi.org/10.1111/j.1365-3032.1962.tb00002.x

King PE, Copland MJW (1969) The structure of the female reproductive system in the Mymaridae (Chalcidoidea: Hymenoptera). Journal of Natural History 3: 349–365. https://doi.org/10.1080/00222936900770311

Kumpanenko AS, Gladun DV (2018) Functional morphology of the sting apparatus of the spider wasp *Cryptocheilus versicolor* (Scopoli, 1763) (Hymenoptera: Pompilidae). Entomological Science 21: 124–132. https://doi.org/10.1111/ens.12288

LeRalec A, Rabasse JM, Wajnberg E (1996) Comparative morphology of the ovipositor of some parasitic Hymenoptera in relation to characteristics of their hosts. Canadian Entomologist 128: 413–433. https://doi.org/10.4039/Ent128413-3

Lösel PD, van de Kamp T, Jayme A, Ershov A, Faragó T, Pichler O, Tan Jerome N, Aadepu N, Bremer S, Chilingaryan SA, Heethoff M, Kopmann A, Odar J, Schmelzle S, Zuber M, Wittbrodt J, Baumbach T, Heuveline V (2020) Introducing Biomedisa as an open-source online platform for biomedical image segmentation. Nature Communications 11: 5577. https://doi.org/10.1038/s41467-020-19303-w

Matushkina NA (2011) Sting microsculpture in the digger wasp *Bembix rostrata* (Hymenoptera, Crabronidae). Journal of Hymenoptera Research 21: 41–52. https://doi.org/10.3897/jhr.21.873

Matushkina NA, Stetsun HA (2016) Morphology of the sting apparatus of the digger wasp *Oxybelus uniglumis* (Linnaeus, 1758) (Hymenoptera, Crabronidae), with emphasis on intraspecific variability and behavioural plasticity. Insect Systematics & Evolution 47: 347–362. https://doi.org/10.1163/1876312X-47032146

Mbata GN, Shapiro-Ilan DI (2010) Compatibility of *Heterorhabditis indica* (Rhabditida: Heterorhabditidae) and *Habrobracon hebetor* (Hymenoptera: Braconidae) for biological control of *Plodia interpunctella* (Lepidoptera: Pyralidae). Biological Control 54: 75–82. https://doi.org/10.1016/j.biocontrol.2010.04.009

Oeser R (1961) Vergleichend-morphologische Untersuchungen über den Ovipositor der Hymenopteren. Mitteilungen aus dem Zoologischen Museum in Berlin 37: 3–119. https://doi.org/10.1002/mmnz.19610370102

Pampel W (1914) Die weiblichen Geschlechtsorgane der Ichneumoniden. Zeitschrift für wissenschaftliche Zoologie 108: 290–357.

Paust A, Reichmuth C, Büttner C, Prozell S, Adler CS, Schöller M (2006) Spatial effects on competition between the larval parasitoids *Habrobracon hebetor* (Say) (Hymenoptera: Braconidae) and *Venturia canescens* (Gravenhorst) (Hymenoptera: Ichneumonidae) parasitising the Mediterranean flour moth, *Ephestia kuehniella* Zeller. Proceedings of the 9th International Working Conference on Stored Product Protection, PS7-17-6189: 797–803.

Peters RS, Krogmann L, Mayer C, Donath A, Gunkel S, Meusemann K, Kozlov A, Podsiadlowski L, Petersen M, Lanfear R, Diez PA, Heraty J, Kjer KM, Klopfstein S, Meier R, Polidori C, Schmitt T, Liu S, Zhou X, Wappler T, Rust J, Misof B, Niehuis O (2017) Evolutionary history of the Hymenoptera. Current Biology 27: 1013–1018. https://doi.org/10.1016/j.cub.2017.01.027

Prozell S, Schöller M, Wyss U (2006) Die Mehlmotte *Ephestia kuehniella* und ihr natürlicher Feind, die Mehlmottenschlupfwespe *Habrobracon hebetor*. Entofilm (Kiel).

Quicke DLJ (1991) Ovipositor mechanics of the braconine wasp genus *Zaglyptogastra* and the ichneumonid genus *Pristomerus*. Journal of Natural History 25: 971–977. https://doi.org/10.1080/00222939100770631

Quicke DLJ (1997) Parasitic Wasps. Chapman & Hall Ltd, London, 470 pp.

Quicke DLJ (2015) The Braconid and Ichneumonid Parasitoid Wasps: Biology, Systematics, Evolution and Eclogy. Wiley-Blackwell, Chichester, 681 pp.

Quicke DLJ, van Achterberg C (1990) Phylogeny of the subfamilies of the family Braconidae (Hymenoptera: Ichneumonoidea). Zoologische Verhandelingen 258: 3–95.

Quicke DLJ, Fitton MG, Ingram S (1992) Phylogenetic implications of the structure and distribution of ovipositor valvilli in the Hymenoptera (Insecta). Journal of Natural History 26: 587–608. https://doi.org/10.1080/00222939200770361

Quicke DLJ, LeRalec A, Vilhelmsen L (1999) Ovipositor structure and function in the parasitic Hymenoptera with an exploration of new hypotheses. Rendiconti 47: 197–239.

Quicke DLJ, Fitton MG, Tunstead JR, Ingram SN, Gaitens PV (1994) Ovipositor structure and relationships within the Hymenoptera, with special reference to the Ichneumonoidea. Journal of Natural History 28: 635–682. https://doi.org/10.1080/00222939400770301

Rahman MH, Fitton MG, Quicke DLJ (1998) Ovipositor internal microsculpture and other features in doryctine wasps (Insecta, Hymenoptera, Braconidae). Zoologica Scripta 27: 333–343. https://doi.org/10.1111/j.1463-6409.1998.tb00465.x

Rogers D (1972) The ichneumon wasp *Venturia canescens*: oviposition and avoidance of superparasitism. Entomologia Experimentalis et Applicata 15: 190–194. https://doi.org/10.1111/j.1570-7458.1972.tb00195.x

Saalfeld S, Fetter R, Cardona A, Tomancak P (2012) Elastic volume reconstruction from series of ultra-thin microscopy sections. Nature Methods 9: 717–720. https://doi.org/10.1038/nmeth.2072

Sanower W, Mbata GN, Payton ME (2018) Improvement of reproductive performance of *Habrobracon hebetor*: Consideration of diapausing and non-diapausing larvae of *Plodia interpunctella*. Biological Control 118: 32–36. https://doi.org/10.1016/j.biocontrol.2017.12.003

Schindelin J, Arganda-Carreras I, Frise E, Kaynig V, Longair M, Pietzsch T, Preibisch S, Rueden C, Saalfeld S, Schmid B, Tinevez J-Y, White DJ, Hartenstein V, Eliceiri K, Tomancak

P, Cardona A (2012) Fiji: an open-source platform for biological-image analysis. Nature Methods 9: 676–682. https://doi.org/10.1038/nmeth.2019

Shah ZA, Blackwell A, Hubbard SF (2012) Ultramorphology of the ovipositor of *Venturia canescens* (Gravenhorst) and possible mechanisms for oviposition. International Journal of Agriculture and Biology 14: 908–914.

Shaw MR (2017) Further notes on the biology of *Pseudavga flavicoxa* Tobias, 1964 (Hymenoptera, Braconidae, Rhysipolinae). Journal of Hymenoptera Research 54: 113–128. https://doi.org/10.3897/jhr.54.10789

Smith EL (1970) Evolutionary morphology of the external insect genitalia. 2. Hymenoptera. Annals of The Entomological Society of America 63: 1–27. https://doi.org/10.1093/aesa/63.1.1

Smith EL (1972) Biosystematics and morphology of Symphyta–III External genitalia of *Euura* (Hymenoptera: Tenthredinidae): sclerites, sensilla, musculature, development and oviposition behavior. International Journal of Insect Morphology and Embryology 1: 321–365. https://doi.org/10.1016/0020-7322(72)90016-5

Snodgrass RE (1933) Morphology of the insect abdomen. Part II. The genital ducts and the ovipositor. Smithsonian Miscellaneous Collections 89: 1–148.

Stetsun H, Matushkina NA (2020) Sting morphology of the European hornet, *Vespa crabro* L., (Hymenoptera: Vespidae) re-examined. Entomological Science 23: 416–429. https://doi.org/10.1111/ens.12438

Stetsun H, Rajabi H, Matushkina N, Gorb SN (2019) Functional morphology of the sting in two digger wasps (Hymenoptera: Crabronidae) with different types of prey transport. Arthropod Structure & Development 52: 100882. https://doi.org/10.1016/j.asd.2019.100882

van Meer NMME, Cerkvenik U, Schlepütz CM, van Leeuwen JL, Gussekloo SWS (2020) The ovipositor actuation mechanism of a parasitic wasp and its functional implications. Journal of Anatomy 237: 689–703. https://doi.org/10.1111/joa.13216

Venkatraman TV, Subba Rao BR (1954) The mechanisms of oviposition in *Stenobracon deesae* (Cam.) (Hymenoptera: Braconidae). Proceedings of the Royal Society of London. Series A, General Entomology 29: 1–8. https://doi.org/10.1111/j.1365-3032.1954.tb01178.x

Vilhelmsen L (2000) The ovipositor apparatus of basal Hymenoptera (Insecta): phylogenetic implications and functional morphology. Zoologica Scripta 29: 319–345. https://doi.org/10.1046/j.1463-6409.2000.00046.x

Vilhelmsen L (2003) Flexible ovipositor sheaths in parasitoid Hymenoptera (Insecta). Arthropod Structure & Development 32: 277–287. https://doi.org/10.1016/S1467-8039(03)00045-8

Vilhelmsen L, Isidore N, Romani R, Basibuyuk HH, Quicke DLJ (2001) Host location and oviposition in a basal group of parasitic wasps: the subgenual organ, ovipositor apparatus and associated structures in the Orussidae (Hymenoptera, Insecta). Zoomorphology 121: 63–84. https://doi.org/10.1007/s004350100046

Währer B, Zimmermann O, Wyss U (2009) Lebensweise und Entwicklung des Parasitoiden *Bracon brevicornis*. Entofim (Kiel).

Yoder MJ, Miko I, Seltmann KC, Bertone MA, Deans AR (2010) A gross anatomy ontology for Hymenoptera. PloS ONE 5: e159991. https://doi.org/10.1371/journal.pone.0015991

Appendix 1

Table A1. Morphological terms relevant to the hymenopteran ovipositor system. The terms (abbreviations used in this article in brackets) are used and defined according to the Hymenoptera Anatomy Ontology Portal (HAO) (Yoder et al. 2010; Hymenoptera Anatomy Consortium 2021) and the according Uniform Resource Identifiers (URI) are listed.

Anatomical term (abbreviation)	definition / concept	URI
1st valvifer (1vf)	The area of the 1st valvifer-1st valvulae complex that is proximal to the aulax, bears the 9th tergal condyle of the 1st valvifer and the 2nd valviferal condyle of the 1st valvifer and is connected to the genital membrane by muscle.	http://purl.obolibrary.org/obo/HAO_0000338
1st valvifer-genital membrane muscle	The ovipositor muscle that arises from the posterior part of the 1st valvifer and inserts anteriorly on the genital membrane anterior to the T9-genital membrane muscle.	http://purl.obolibrary.org/obo/HAO_0001746
1st valvula, 1st valvulae (1vv)	The area of the 1st valvifer-1st valvulae complex that is delimited by the proximal margin of the aulax.	http://purl.obolibrary.org/obo/HAO_0000339
2nd valvifer (2vf)	The area of the 2nd valvifer-2nd valvulae-3rd valvulae complex that is proximal to the basal articulation and to the processus musculares and articulates with the female T9.	http://purl.obolibrary.org/obo/HAO_0000927
2nd valvula (2vv)	The area of the 2nd valvifer-2nd valvulae-3rd valvulae complex that is distal to the basal articulation and to the processus musculares and is limited medially by the median body axis.	http://purl.obolibrary.org/obo/HAO_0000928
3rd valvula, 3rd valvulae (3vv)	The area of the 2nd valvifer-3rdvalvulae complex that is posterior to the distal vertical conjunctiva of the 2nd valvifer-3rd valvulae complex.	http://purl.obolibrary.org/obo/HAO_0001012
anterior 2nd valvifer-2nd valvula muscle	The ovipositor muscle that arises from the anterodorsal part of the 2nd valvifer and inserts subapically on the processus articularis.	http://purl.obolibrary.org/obo/HAO_0001166
anterior ridge of T9 (ar9)	The ridge that extends along the anterior margin of female T9 and receives the site of origin of the ventral and the dorsal T9-2nd valvifer muscles.	http://purl.obolibrary.org/obo/HAO_0002182
anterior section of dorsal flange of 2nd valvifer	The area of the dorsal flange of the 2nd valvifer that is anterior to the site of origin of the basal line.	http://purl.obolibrary.org/obo/HAO_0002173
apodeme	The process that is internal.	http://purl.obolibrary.org/obo/HAO_0000142
aulax (au)	The impression that is on the 1st valvifer-1st valvula complex accommodates the rhachis.	http://purl.obolibrary.org/obo/HAO_0000152
basal articulation (ba)	The articulation that is part of the 2nd valvifer-2nd valvula-3rd valvula complex and adjacent to the rhachis.	http://purl.obolibrary.org/obo/HAO_0001177
basal line of the 2nd valvifer	The line on the 2nd valvifer that extends between the pars articularis and the dorsal flange of 2nd valvifer.	http://purl.obolibrary.org/obo/HAO_0002171
bulb (blb)	The anterior area of the dorsal valve [composite structure of the fused 2nd valvulae] that is bulbous.	http://purl.obolibrary.org/obo/HAO_0002177
conjunctiva	The area of the cuticle that is more flexible than adjacent sclerites.	http://purl.obolibrary.org/obo/HAO_0000221
distal notch of the dorsal valve (no)	The notch that is distal on the dorsal valve [composite structure of the fused 2nd valvulae].	http://purl.obolibrary.org/obo/HAO_0002179
dorsal flange of the 2nd valvifer (df2)	The flange that extends on the dorsal margin of the 2nd valvifer. Part of the ventral T9-2nd valvifer muscle attaches to the flange.	http://purl.obolibrary.org/obo/HAO_0001577
dorsal projection of the 2nd valvifer (dp2)	The projection that is located on the 2nd valvifer and corresponds to the proximal end of the rhachis.	http://purl.obolibrary.org/obo/HAO_0002172
dorsal ramus of the 1st valvula (dr1)	The region that extends along the dorsal margin of the 1st valvula and bears the aulax.	http://purl.obolibrary.org/obo/HAO_0001579
dorsal T9-2nd valvifer muscle	The ovipositor muscle that arises along the posterodorsal part of the anterior margin of female T9 and inserts on the anterior section of the dorsal flanges of the 2nd valvifer.	http://purl.obolibrary.org/obo/HAO_0001569
egg canal (ec)	The anatomical space that is between the left and right olistheters.	http://purl.obolibrary.org/obo/HAO_0002191
female T9 (T9)	The tergite that is articulated with the 1st valvifer and is connected to the 2nd valvifer via muscles.	http://purl.obolibrary.org/obo/HAO_0000075
flange	The projection that is lamella-like and is located on a rim, carina, apodeme or edge.	http://purl.obolibrary.org/obo/HAO_0000344
genital membrane (gm)	The conjunctiva that connects the ventral margins of the 2nd valvifers arching above the 2nd valvula.	http://purl.obolibrary.org/obo/HAO_0001757

Anatomical term (abbreviation)	definition / concept	URI
interarticular ridge of the 1st valvifer (iar)	The ridge that extends along the posterior margin of the 1st valvifer between the intervalvifer and tergo-valvifer articulations.	http://purl.obolibrary.org/obo/HAO_0001562
intervalvifer articulation (iva)	The articulation between the 1st valvifer and 2nd valvifer.	http://purl.obolibrary.org/obo/HAO_0001558
median bridge of the 2nd valvifers (mb2)	The area that connects posterodorsally the 2nd valvifers and is the site of attachment for the posterior T9-2nd valvifer muscle.	http://purl.obolibrary.org/obo/HAO_0001780
notal membrane	The conjunctiva that connects the medial margins of the 2nd valvulae.	http://purl.obolibrary.org/obo/HAO_0001733
notch	The part of the margin of a sclerite that is concave.	http://purl.obolibrary.org/obo/HAO_0000648
olistheter (oth)	The anatomical cluster that is composed of the rhachis of the 2nd valvula and the aulax of the 1st valvula.	http://purl.obolibrary.org/obo/HAO_0001103
ovipositor	The anatomical cluster that is composed of the 1st valvulae, 2nd valvulae, 3rd valvulae, 1st valvifers, 2nd valvifers and female T9.	http://purl.obolibrary.org/obo/HAO_0000679
ovipositor apparatus	The anatomical cluster that is composed of the ovipositor, abdominal terga 8-10, abdominal sternum 7 and muscles connecting them.	http://purl.obolibrary.org/obo/HAO_0001600
ovipositor muscle	The abdominal muscle that inserts on the ovipositor.	http://purl.obolibrary.org/obo/HAO_0001290
pars articularis / pars articulares	The articular surface that is situated anteriorly on the ventral margin of the 2nd valvifer and forms the lateral part of the basal articulation.	http://purl.obolibrary.org/obo/HAO_0001606
posterior 2nd valvifer-2nd valvula muscle	The ovipositor muscle that arises posteroventrally from the 2nd valvifer and inserts on the processus musculares of the 2nd valvula.	http://purl.obolibrary.org/obo/HAO_0001815
processus articularis / processus articulares	The process that extends laterally from the proximal part of the 2nd valvula and forms the median part of the basal articulation, and corresponds to the site of attachment for the anterior 2nd valvifer-2nd valvula muscle. The processus articularis is part of the sclerite.	http://purl.obolibrary.org/obo/HAO_0001704
processus musculares / processus muscularis	The apodeme that extends dorsally from the proximal part of the 2nd valvula to the genital membrane and receives the site of attachment of the posterior 2nd valvifer-2nd valvula muscle.	http://purl.obolibrary.org/obo/HAO_0001703
rhachis (rh)	The ridge that extends along the ventral surface of the 2nd valvula that is partially enclosed by the aulax.	http://purl.obolibrary.org/obo/HAO_0000898
ridge	The apodeme that is elongate.	http://purl.obolibrary.org/obo/HAO_0000899
sawtooth (st)	The process that is located along the ventral margin of the 1st valvula of the dorsal margin of the 2nd valvula.	http://purl.obolibrary.org/obo/HAO_0001681
sclerite	The area of the cuticle that is less flexible than adjacent conjunctivae.	http://purl.obolibrary.org/obo/HAO_0000909
sensillar patch of the 2nd valvifer (sp)	The patch that is composed of placoid sensilla adjacent to the intervalvifer articulation.	http://purl.obolibrary.org/obo/HAO_0001671
sensillum	A sense organ embedded in the integument and consisting of one or a cluster of sensory neurons and associated sensory structures, support cells and glial cells forming a single organized unit with a largely bona fide boundary.	http://purl.obolibrary.org/obo/HAO_0000933
terebra (trb)	The anatomical cluster that is composed of the 1st and 2nd valulae.	http://purl.obolibrary.org/obo/HAO_0001004
tergite	The sclerite that is located on the tergum.	http://purl.obolibrary.org/obo/HAO_0001005
tergo-valvifer articulation (tva)	The articulation that is located between the female T9 and the 1st valvifer and is composed of the 9th tergal condyle of the 1st valvifer and the 1st valviferal fossa of the 9th tergite.	http://purl.obolibrary.org/obo/HAO_0001636
valvillus (vlv)	The sclerite that articulates on the 1st valvula and projects into the egg/poison canal.	http://purl.obolibrary.org/obo/HAO_0001619
venom gland reservoir of the 2nd valvifer (vd)	The gland reservoir that is between the 2nd valvifers.	http://purl.obolibrary.org/obo/HAO_0002176
ventral ramus of the 2nd valvula	The area of the 2nd valvifer-2nd valvula-3rd valvula complex that bears the rhachis.	http://purl.obolibrary.org/obo/HAO_0001107
ventral T9-2nd valvifer muscle	The ovipositor muscle that arises from the lateral region of female T9 and inserts along the posterior part of the dorsal flange of the 2nd valvifer.	http://purl.obolibrary.org/obo/HAO_0001616

Supplementary material 1

Video S1

Authors: Michael Csader, Karin Mayer, Oliver Betz, Stefan Fischer, Benjamin Eggs

Data type: Video file (mp4)

Explanation note: Animation of the rotated segmented 3D reconstruction of the terebra of *Habrobracon hebetor*.

Copyright notice: This dataset is made available under the Open Database License (http://opendatacommons.org/licenses/odbl/1.0/). The Open Database License (ODbL) is a license agreement intended to allow users to freely share, modify, and use this Dataset while maintaining this same freedom for others, provided that the original source and author(s) are credited.

Link: https://doi.org/10.3897/jhr.83.64018.suppl1

Supplementary material 2

Video S2

Authors: Michael Csader, Karin Mayer, Oliver Betz, Stefan Fischer, Benjamin Eggs

Data type: Video file (mp4)

Explanation note: Animation of the rotated segmented 3D reconstruction of the proximal region of the terebra of *Habrobracon hebetor* (cf. Fig. 3), highlighting the 1st and 2nd valvulae, the ligaments, and the duct of the venom gland.

Copyright notice: This dataset is made available under the Open Database License (http://opendatacommons.org/licenses/odbl/1.0/). The Open Database License (ODbL) is a license agreement intended to allow users to freely share, modify, and use this Dataset while maintaining this same freedom for others, provided that the original source and author(s) are credited.

Link: https://doi.org/10.3897/jhr.83.64018.suppl2